SANDIA REPORT
SAND2008-6687
Unlimited Release
Printed October 2008

Computational Investigation of Noble Gas Adsorption and Separation by Nanoporous Materials

Jeffery A. Greathouse, Mark D. Allendorf, and Joseph C. Sanders

Prepared by
Sandia National Laboratories
Albuquerque, New Mexico 87185 and Livermore, California 94550

Sandia is a multiprogram laboratory operated by Sandia Corporation,
a Lockheed Martin Company, for the United States Department of Energy's
National Nuclear Security Administration under Contract DE-AC04-94AL85000.

Issued by Sandia National Laboratories, operated for the United States Department of Energy by Sandia Corporation.

Available to DOE and DOE contractors from
U.S. Department of Energy
Office of Scientific and Technical Information
P.O. Box 62
Oak Ridge, TN 37831

Telephone: (865) 576-8401
Facsimile: (865) 576-5728
E-Mail: reports@adonis.osti.gov
Online ordering: http://www.osti.gov/bridge

Available to the public from
U.S. Department of Commerce
National Technical Information Service
5285 Port Royal Rd.
Springfield, VA 22161

Telephone: (800) 553-6847
Facsimile: (703) 605-6900
E-Mail: orders@ntis.fedworld.gov
Online order: http://www.ntis.gov/help/ordermethods.asp?loc=7-4-0#online

SAND2008-6687
Unlimited Release
Printed October 2008

Computational Investigation of Noble Gas Adsorption and Separation by Nanoporous Materials

Jeffery A. Greathouse
Geochemistry Department
Sandia National Laboratories
P.O. Box 5800, MS 0754
Albuquerque, New Mexico, 87185-0754

Mark D. Allendorf
Microfluidics Department
Sandia National Laboratories
P.O. Box 969
Livermore, California 94550

Joseph C. Sanders
Systems Analysis Department
Sandia National Laboratories
P.O. Box 5800, MS 1218
Albuquerque, New Mexico, 87185-1218

Abstract

Molecular simulations are used to assess the ability of metal-organic framework (MOF) materials to store and separate noble gases. Specifically, grand canonical Monte Carlo simulation techniques are used to predict noble gas adsorption isotherms at room temperature. Experimental trends of noble gas inflation curves of a Zn-based material (IRMOF-1) are matched by the simulation results. The simulations also predict that IRMOF-1 selectively adsorbs Xe atoms in Xe/Kr and Xe/Ar mixtures at total feed gas pressures of 1 bar (14.7 psia) and 10 bar (147 psia). Finally, simulations of a copper-based MOF (Cu-BTC) predict this material's ability to selectively adsorb Xe and Kr atoms when present in trace amounts in atmospheric air samples. These preliminary results suggest that Cu-BTC may be an ideal candidate for the pre-concentration of noble gases from air samples. Additional simulations and experiments are needed to determine the saturation limit of Cu-BTC for xenon, and whether any krypton atoms would remain in the Cu-BTC pores upon saturation.

Contents

Figures

Tables

1. INTRODUCTION

Metal organic frameworks (MOFs) are a recently created class of nanoporous materials whose pore size and chemical environment can be chemically tailored because of the hybrid inorganic/organic nature of their structure [1]. Known as coordination polymers, MOFs consist of metal ions connected to each other through bridging organic "linker" molecules that coordinate to the metal centers. Figure 1.1 compares the structure of a zeolite (mordenite) with IRMOF-1 (zinc benzene dicarboxylate), a prototype material used in many benchmark studies of MOFs. The isoreticular series of zinc- and copper-based IRMOF (isoreticular metal-organic framework) compounds [2-4] are of particular interest because of their potential for rational design of nanoporous materials, enabled by the inherent synthetic versatility of the linker molecule. Although a seemingly vast array of possibilities for creating MOFs with specific properties would seem to exist, neither the properties resulting from the choice of a particular linker, nor the ability to synthesize a MOF from it can be considered a certainty. Thus, there is an important role for theoretical methods that can predict properties such as molecular diffusion and adsorption, enabling the most promising candidates to be identified prior to launching a potentially time-consuming synthetic effort. Atomistic methods, such as molecular dynamics and Monte Carlo techniques, are particularly attractive for this purpose, due to their ability to evaluate a wide variety of related chemical systems, and their compatibility with high-performance computing systems [5].

Several properties of both mordenite and IRMOF-1 are compared in Table 1.1. Mordenite has one of the largest free apertures known to zeolites, but the IRMOF-1 aperture is much larger. As a result, gas diffusivity should be at least 100 times greater in IRMOF-1, which should result in faster and cheaper pressure-swing adsorption processes. The density of MOFs is also much lower than zeolites, due to their large pores. MOFs should therefore be lighter and more portable than zeolites. The final property (surface area) has resulted in significant industrial attention being paid to MOFs. They have the highest surface area and the greatest gas adsorption capacity of any known crystalline material. These comparisons suggest that IRMOF-1 or other MOF materials can be designed with superior gas adsorption and separation properties compared to the best zeolites.

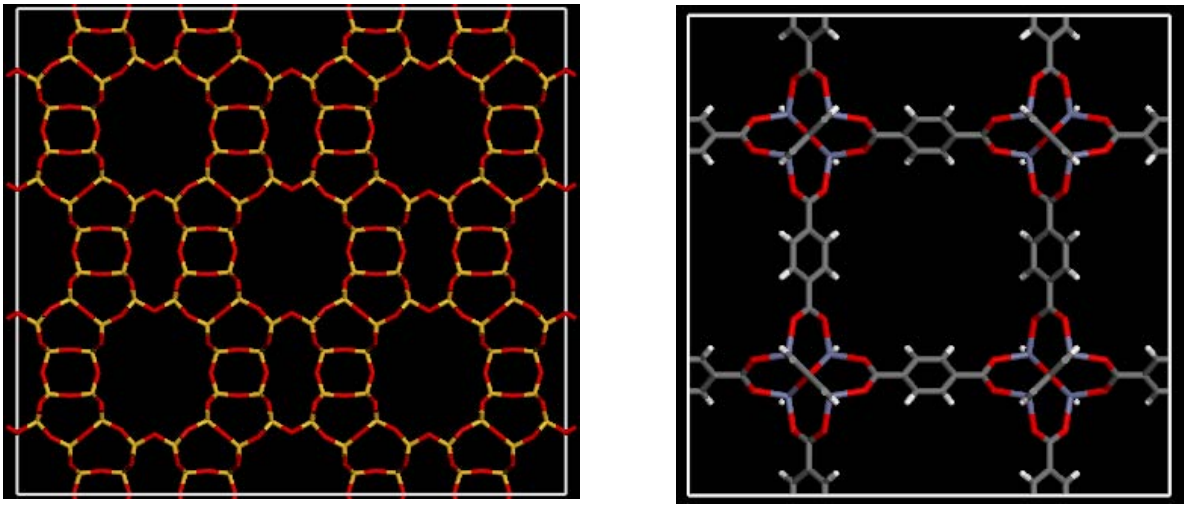

Figure 1.1 Molecular structures of a representative zeolite (mordenite, left) and a MOF (IRMOF-1, zinc benzene dicarboxylate, right). Mordenite is composed of silica (SiO_2) units, while IRMOF-1 is composed of Zn_4O clusters connected by benzene dicarboxylate (BDC) linkers. Si atoms are yellow, O atoms are red, Zn atoms are blue, C atoms are gray, and H atoms are white).

Table 1.1. Physical properties of zeolites (mordenite) and MOFs (IRMOF-1).

property	mordenite	IRMOF-1
Pore Apertures	6.7 Å x 7.0 Å 2.9 Å x 5.7 Å	11.2 Å x 11.2 Å
Density	1.6 g cm^{-3}	0.6 g cm^{-3}
Surface Area	300 m^2 g^{-1}	3500 m^2 g^{-1}

The industrial applications of MOFs have recently been reviewed [6]. In particular, Mueller et al. showed that a copper-containing MOF known as Cu-BTC (BTC = benzene tricarboxylate) can separate Xe from Kr (Figure 1.2) with a selectivity factor of 1200. This extremely high separation factor indicates Cu-BTC is a highly efficient material for concentrating trace components. Note that in this case, the open channels are ~ 1 nm (10 Å) diameter, which is considerably larger than the kinetic diameters of Xe (4.0 Å) and Kr (3.6 Å). Thus, the selectivity is not based upon size alone, but results from a combination of size, high surface area, and the favorable electronic (van der Waals) interaction between the gas and the channel walls. MOFs are sufficiently stable that they can be heated to temperatures as high as 300 °C in air, enabling trapped gases to be efficiently desorbed. Thus, MOFs are attractive for many applications involving purification, separation, or storage of noble gases.

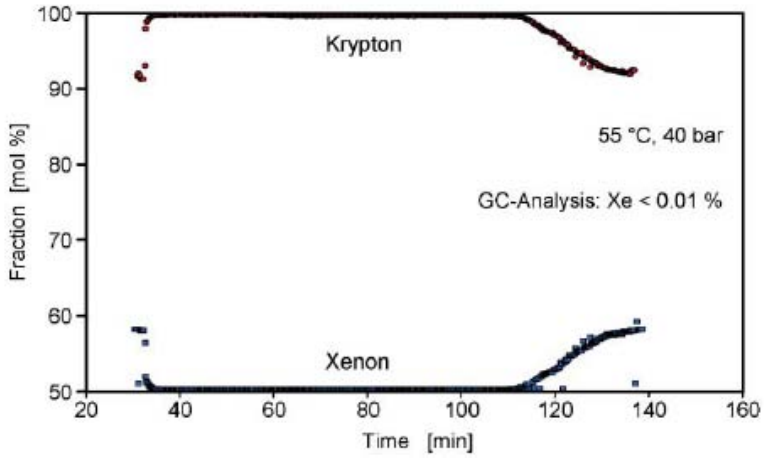

Figure 1.2. Gas separation of Kr-Xe mixture by continuous adsorption on electrochemically produced Cu-BTC [6]. The input stream consisted of 94 mol% Kr and 6 mol% (60,000 ppm) Xe at 40 bar (588 psia) pressure, over 193 g of Cu-BTC (60 L/h flow rate). Shortly after exposure, analysis by gas chromatography (GC) shows that the Xe concentration was reduced to 50 ppm. Reproduced by permission from the Royal Society of Chemistry, http://dx.doi.org/10.1039/b511962f.

Our goal in this project is to use computational techniques to determine the ability of MOF materials to capture and preconcentrate noble gases from air samples. Specifically, grand canonical Monte Carlo simulations are used to simulate the loading of adsorbate gases within the porous frameworks. Using our molecular modeling force field for Zn-based MOFs, we compare simulated noble gas compression curves with experimental results. We also show that IRMOF-1 has a high selectivity for Xe in Xe/Ar and Xe/Kr mixtures. Finally, we show that a Cu-based MOF (Cu-BTC) selectively adsorbs Xe and Kr when present in trace amounts in air samples.

2. MODELING METHODS

The Towhee code (http://towhee.sourceforge.net) was used to perform grand canonical Monte Carlo (GCMC) simulations of gas adsorption by MOF materials. Thermodynamic input parameters include the temperature T (292 K – 300 K), host (MOF) volume V, and guest chemical potential μ. A Monte Carlo move consists of one of the following: translation of a guest or host molecule, rotation of a host molecule, insertion of a new guest molecule, or deletion of an existing guest molecule. Rotation moves are not necessary for spherical guest particles. The total potential energy is calculated from a classical energy expression governed by pairwise potential parameters in the form of a force field. Parameters for the noble gas guests were taken from the literature [7, 8]. The simulation box consists of one unit cell of the MOF (IRMOF-1 or Cu-BTC), with atomic positions taken from their crystal structures. The Towhee code requires adsorbate chemical potentials rather than feed gas fugacity as input, so we performed "empty box" GCMC simulations (i.e., a box without the MOF unit cell) to establish appropriate chemical potentials for the guest target pressures [9].

2.1 IRMOF-1 Simulations

We have developed a hybrid force field for IRMOF-1, which includes nonbonded interactions between Zn atoms, inorganic O atoms, and benzene dicarboxylate (BDC) linkers. The original nonbonded parameters [10] were derived from the Consistent Valence Force Field (CVFF) [11] and parameters optimized for the mineral zincite (ZnO), but they were recently modified by Dubbeldam et al. to reproduce CO_2 and CH_4 adsorption isotherms [12]. Unlike the implementation we used for molecular dynamics simulations [10], in which the linker molecules are fully flexible (bond, angle, torsion), here we use a semi-flexible approach where the BDC linkers are treated as rigid structures. Test simulations in which linker flexibility was included by a torsional pivot move gave similar results to the semi-flexible force field. First, single component adsorption isotherms are obtained for argon, krypton, and xenon for feed gas pressures up to 40 bar. Second, xenon selectivity by IRMOF-1 is determined from xenon/argon and xenon/krypton feed gas mixtures at total pressures of 1 bar and 10 bar. A total of 8 million MC moves are used for the simulations, and the last 5 million moves are used for averaging and analysis.

2.2 Cu-BTC Simulations

The framework is treated as a rigid body, and force field parameters are taken from the literature [13]. Separate parameters were reported for Cu-BTC atoms depending on the type of guest molecules (oxygen or nitrogen). Our simulations contain both guests, so an arithmetic average of the two Cu-BTC parameter sets is used. In addition to nitrogen and oxygen guests with gas-phase mole fractions of 0.8 and 0.2, respectively, krypton and xenon guests are included in trace concentrations. Due to the low guest concentrations, a total of 35 million GCMC moves are used for the simulations, and the last 30 million moves are used for averaging and analysis. Initially, chemical potentials for krypton and xenon were chosen to correspond to their natural abundances

in air (1.1 ppm and 0.087 ppm, respectively). However, the GCMC insertion/deletion statistics were so low at these concentrations, that the simulations were repeated at higher krypton and xenon concentrations (2200 ppm and 166 ppm, respectively). We note that the ratio of abundances (Kr/Xe) in the second set is similar to the ratio of natural abundances. All Cu-BTC simulations were performed at a temperature of 300 K.

3. RESULTS

3.1 Adsorption and selectivity of noble gases by IRMOF-1

First, we simulated a well-known Zn-based MOF, which has a high storage capacity for noble gases – Figure 3.1 compares our simulated Xe adsorption isotherm for IRMOF-1 with experimental data collected at 292 K. There is good agreement at low pressure, but at higher pressures the simulation underpredicts the experimental Xe loading. A snapshot from the simulation (Figure 3.2) indicates that there is no preferred binding site for Xe atoms within the IRMOF-1 lattice at room temperature. While this behavior differs from that predicted for light gas adsorption by IRMOF-1 at 30 K, in which the zinc-oxygen clusters are the preferred binding sites, it is consistent with room temperature predictions for this adsorbent [14]. Furthermore, Figure 3.2 is consistent with ^{129}Xe nuclear magnetic resonance (NMR) spectra at room temperature, indicating that Xe atoms occupy all possible adsorption sites within the IRMOF-1 pore [15].

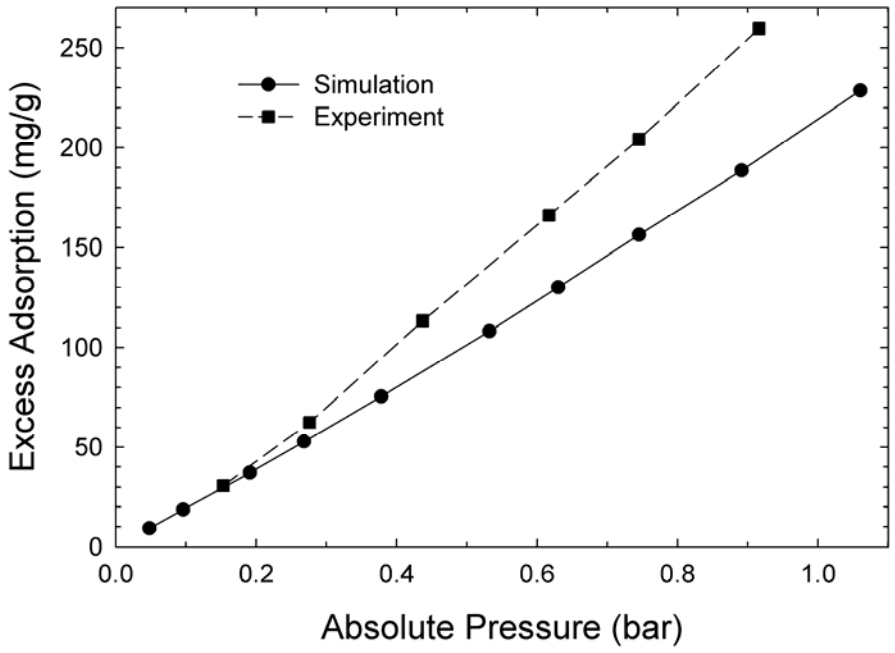

Figure 3.1. Xenon adsorption isotherms for IRMOF-1 at 292 K, comparing simulation and experiment [15].

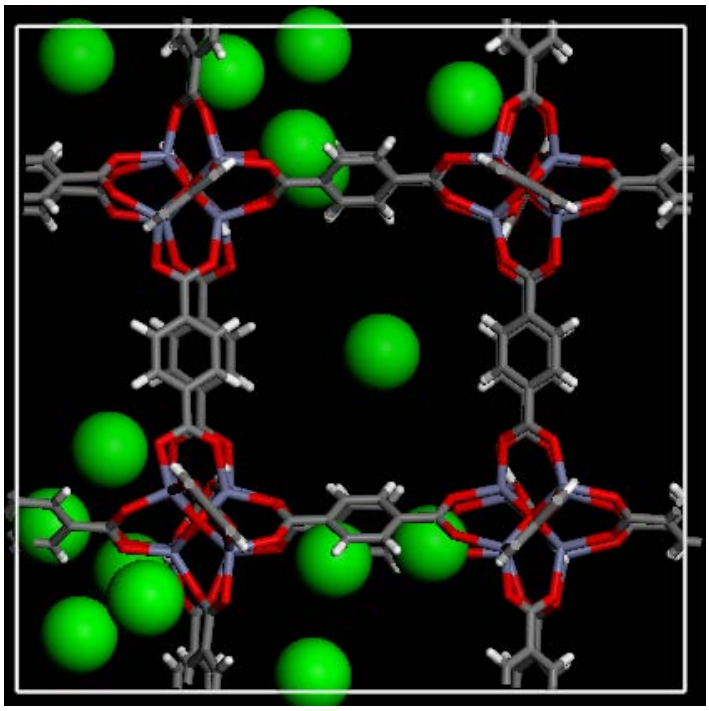

Figure 3.2. Snapshot of IRMOF-1, with adsorbed xenon atoms shown in green.

The ability of IRMOF-1 to store noble gases at much higher densities than the corresponding "empty containers" has been demonstrated experimentally. Corresponding GCMC simulation results are presented in Figure 3.3 for comparison. The agreement between the empty container compression curves (red lines in Figure 3.3) and the experimental results is excellent, suggesting that the van der Waals parameters correctly describe the gas-gas interactions for compressed Ar, Kr, and Xe. The simulated inflation curves (blue lines in Figure 3.3) show qualitatively that significant additional amounts of each gas can be stored in the same container filled with IRMOF-1. As usual, the simulation results overpredict the adsorption isotherms, but for this specific comparison two comments are in order. First, the simulations involve perfectly crystalline IRMOF-1, while the "*in situ* activated MOF sample" used experimentally [6] almost certainly contained defects that would have reduced the surface area. Second, the simulated container has the dimensions of exactly one unit cell of IRMOF-1, while the experimental container could not have been completely filled with IRMOF-1 and therefore contained some empty space.

IRMOF-1 exhibits preferential adsorption for Xe over the smaller noble gases Kr and Ar (Figure 3.4). The selectivity for Xe, and the pressure dependence of Xe selectivity, is greatly enhanced when Xe is mixed with smaller atoms (Ar) compared with larger atoms (Kr). However, even smaller selectivities seen in the Xe/Kr mixtures (2.5 – 3.0) lead to an effective separation of the gases. At low feed concentrations of Xe (e.g., 10% Xe, 90% Kr), the adsorbed phase consists of 38% Xe and 62% Kr.

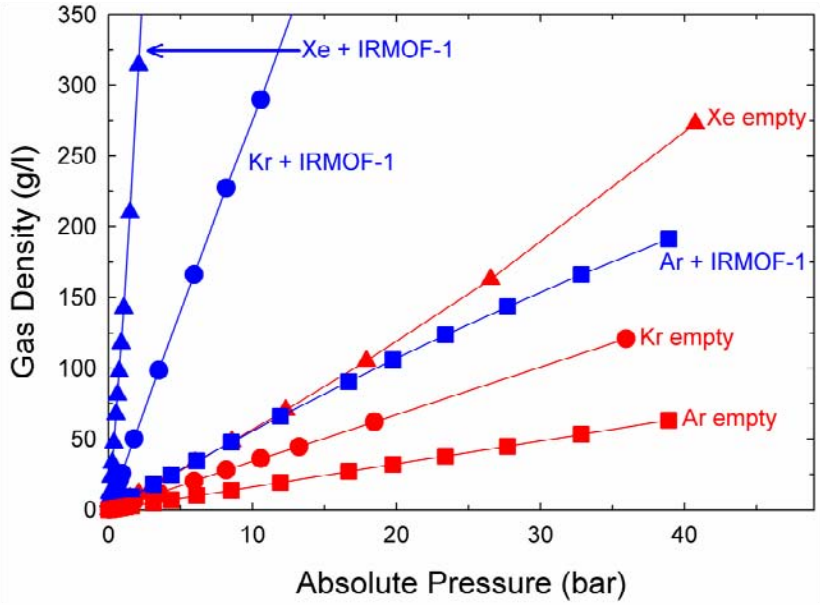

Figure 3.3. Simulated compression curves for noble gases in empty containers (red), compared with inflation curves (blue) in the presence of IRMOF-1 at 300 K. The blue curves represent total gas adsorption, not excess adsorption, for comparison with experimental results [6].

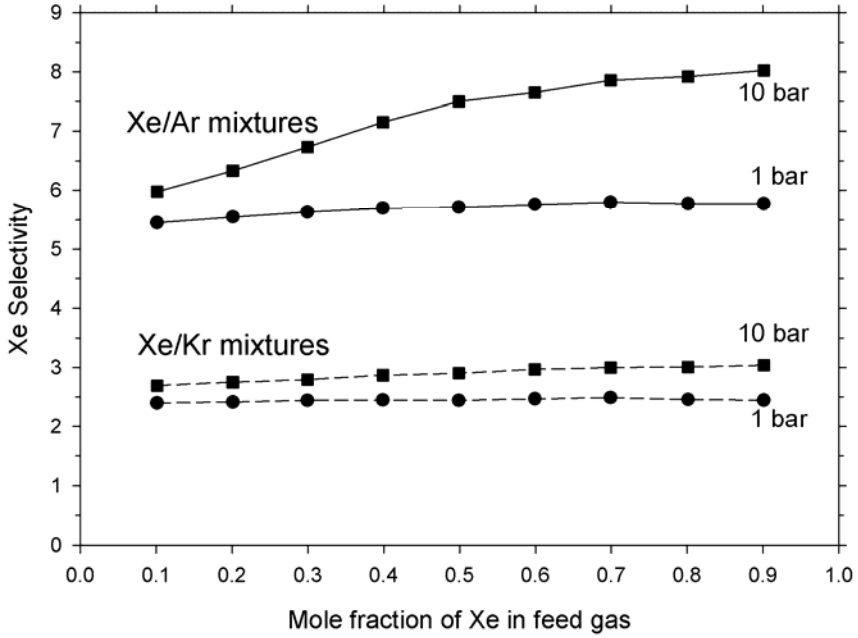

Figure 3.4. Effect of feed gas composition on Xe selectivity for Xe/Ar mixtures (solid lines) and Xe/Kr mixtures (dashed lines) at 300 K and total feed pressures of 1.0 bar and 10.0 bar.

3.2 Simulations of noble gas adsorption by Cu-BTC in air

The second part of the project involves a Cu-based MOF, Cu-BTC. Table 3.1 summarizes the guest insertion/deletion statistics from the simulations, as well as guest mole fractions in the adsorbed phase. Using the natural abundances for krypton and xenon, which are very low, reliable adsorption data cannot be obtained from the poor swap statistics. By increasing the krypton and xenon abundances by several orders of magnitude, statistically valid results are obtained. In future work, increasing both the number of Monte Carlo moves and simulation cell size may allow us to simulate these gases at their natural abundances.

Table 3.1. Summary of Cu-BTC simulations at 300 K: Xe and Kr insertion/deletion statistics and guest mole fractions in the adsorbed phase.

y (Xe)[a]	*y* (Kr)[a]	Xe swap moves[b]	Kr swap moves[b]
8.70×10^{-8}	1.10×10^{-6}	8	20
1.66×10^{-4}	2.20×10^{-3}	9709	30945

[a] *y* refers to the guest mole fraction in the pure gas phase (i.e., without the MOF).
[b] A swap move is defined as either a guest insertion or a guest deletion.

The amount of each guest adsorbed by Cu-BTC is compared to its feed gas abundance in Table 3.2. The mole fraction data do not reflect the total gas density in each phase. The gas-phase, system (26.343 Å x 26.343 Å x 26.343 Å) contained an average of 0.44 molecules total, which is much less than the 1.86 molecules in the same volume filled with Cu-BTC. The average gas density increases by a factor of 4.2 in the presence of Cu-BTC, and this ratio is similar to the compression ratios of nitrogen and oxygen in Table 3.2. The compression ratios for krypton (16.9) and xenon (71.0) are much larger, suggesting that Cu-BTC shows preferential adsorption of these noble gases in the presence of air. Additionally, the very large compression ratio for xenon compared to krypton is consistent with the selectivity of xenon by Cu-BTC seen experimentally (Figure 1.2).

Table 3.2. Guest adsorption results from Cu-BTC simulations at 300 K.

guest	*y* (gas)[a]	*x* (CuBTC)[b]	compression ratio (# adsorbed / # gas)
N_2	0.797	0.773	4.1
O_2	0.200	0.215	4.5
Xe	1.66×10^{-4}	2.80×10^{-3}	71.0
Kr	2.20×10^{-3}	8.87×10^{-3}	16.9

[a] *y* refers to the guest mole fraction in the pure gas phase.
[b] *x* refers to the guest mole fraction in the adsorbed phase (Cu-BTC pore).
[c] The compression ratio indicates the increase in guest occupancy in the same system volume containing Cu-BTC compared to the pure gas phase (no Cu-BTC).

4. CONCLUSIONS

The results from this proof-of-concept project clearly demonstrate that molecular modeling can be used to explain the observed gas adsorption and separation properties of MOF materials, and to predict undiscovered properties. Furthermore, the practicality of tailoring MOFs to absorb certain species more effectively than zeolites, including mordenite, is clear. The trend in simulated noble gas adsorption isotherms for IRMOF-1 (Figure 3.3) is in excellent agreement with published experimental results. Additional simulations and experiments are needed to determine the saturation limit of Cu-BTC for xenon, and whether any krypton atoms would remain in the Cu-BTC pores upon saturation. The results for xenon and krypton adsorption by Cu-BTC in the presence of air demonstrate the exciting potential for MOFs as a sorbent material in nonproliferation applications, and the potential of achieving higher gas adsorption per unit MOF mass or volume relative to zeolites.

Future modeling work in this area should be coupled with adsorption experiments for validation. Specific action items include: 1) the effect of water vapor on noble gas adsorption and separation; 2) adsorption under various temperature conditions (both above and below STP); 3) the effect of pre-concentrating air samples prior to adsorption; 4) regeneration conditions for the bed material; and 5) the ability to absorb xenon and krypton directly from air at their respective mole fractions.

REFERENCES

1. M. Eddaoudi, J. Kim, N. Rosi, D. Vodak, J. Wachter, M. O'Keefe, and O. M. Yaghi, Science 295:469 (2002).
2. J. L. C. Rowsell and O. M. Yaghi, Microporous and Mesoporous Materials 73:3 (2004).
3. G. Ferey, C. Mellot-Draznieks, C. Serre, F. Millange, J. Dutour, S. Surble, and I. Margiolake, Science 309:2040 (2005).
4. S. Surble, C. Serre, C. Mellot-Draznieks, F. Millange, and G. Ferey, Chemical Communications:284 (2006).
5. D. Dubbeldam and R. Q. Snurr, Molecular Simulation 33:305 (2007).
6. U. Mueller, M. Schubert, F. Teich, H. Puetter, K. Schierle-Arndt, and J. Pastre, Journal of Materials Chemistry 16:626 (2006).
7. J. O. Hirschfelder, C. F. Curtiss, and R. B. Bird, Molecular Theory of Gases and Liquids, Wiley, New York, 1965.
8. G. C. Maitland, M. Rigby, E. B. Smith, and W. A. Wakeham, Intermolecular Forces: Their Origin and Determination, Clarendon Press, Oxford, U.K., 1981.
9. T. M. Nicholson and S. K. Bhatia, Adsorption Science & Technology 25:607 (2007).
10. J. A. Greathouse and M. D. Allendorf, Journal of Physical Chemistry C 112:5795 (2008).
11. P. Dauber-Osguthorpe, V. A. Roberts, D. J. Osguthorpe, J. Wolff, M. Genest, and A. T. Hagler, Proteins: Structure, Function, and Genetics 4:31 (1988).
12. D. Dubbeldam, K. S. Walton, D. E. Ellis, and R. Q. Snurr, Angewandte Chemie International Edition 46:4496 (2007).
13. Q. Y. Yang, C. Y. Xue, C. L. Zhong, and J. F. Chen, Aiche Journal 53:2832 (2007).
14. D. Dubbeldam, H. Frost, K. S. Walton, and R. Q. Snurr, Fluid Phase Equilibria 261:152 (2007).
15. S. Pawsey, I. Moudrakovski, J. Ripmeester, L. Q. Wang, G. J. Exarhos, J. L. C. Rowsell, and O. M. Yaghi, Journal of Physical Chemistry C 111:6060 (2007).

Distribution

1	Les Pitts, DOE/NNSA/NA-22	
1	Leslie Casey, DOE/NNSA/NA-22	
1	Eleanor Dixon, DOE/NNSA/NA-22	
1	MS 1209	G. L. Laughlin, 5920
3	MS 1218	J. C. Sanders, 5924
3	MS 0754	J. A. Greathouse, 6316
1	MS 0754	M. J. Rigali, 6316
1	MS 9004	W. P. Ballard, 8100
1	MS 9004	B. K. Damkroger, 8130
1	MS 9004	J. M. Hruby, 8100
1	MS 9291	M. D. Allendorf, 8324
1	MS 9291	M. M. Young, 8324
1	MS 9402	J. E. M. Goldsmith, 8772
1	MS 9402	F. P. Doty, 8772
1	MS 9406	J. C. Lund, 8132
1	MS 0899	Technical Library, 9536 (electronic copy)


Sandia National Laboratories